

Magnetic and Photocatalytic Behaviors of Ca Mn Co-Doped BiFeO₃ Nanofibres

Yannan Feng, Huanchun Wang, Yang Shen, Yuanhua Lin*, Cewen Nan

State Key Laboratory of New Ceramics and Fine Processing, School of Materials Science and Engineering, Tsinghua University, Beijing, China
Email: *linyh@tsinghua.edu.cn

Received May 29, 2013; revised June 29, 2013; accepted August 1, 2013

Copyright © 2013 Yannan Feng *et al.* This is an open access article distributed under the Creative Commons Attribution License, which permits unrestricted use, distribution, and reproduction in any medium, provided the original work is properly cited.

ABSTRACT

Ca and Mn co-doped BiFeO₃ ultrafine nanofibres were prepared with the purpose of improving magnetic and photocatalytic performances of the one-dimensional multiferroic material. Impurity phase introduced by both Bi fluctuation and Mn substitution can be suppressed by Ca doping and a space group transition from R3c to C222 can also be triggered by Bi-site doping. With co-substitution of Mn into iron site, the Ca_{0.15}Bi_{0.85}Mn_{0.05}Fe_{0.95}O₃ nanofibres presented a larger saturation magnetization than the singly Ca doping samples, possibly due to the increased double exchange interaction of Fe³⁺-O-Fe²⁺, strengthened by Ca and Mn. Photocatalytic degradation test witnessed a similar drop-and-rise performance with the magnetism.

Keywords: Bismuth Ferrite; Nanofibre; Magnetic; Photocatalytic

1. Introduction

Bismuth ferrite (BiFeO₃, or BFO), one of the most widely researched multiferroics, has continuously proved to be a remarkable attraction, due to its room temperature antiferromagnetic and ferroelectric orderings, [1] high visible light response, and consequent potentiality in multifunctional devices [2,3] and polluted water remediation [4]. In order to promote the performance of BFO, a variety of nanostructures have been fabricated [5-7] and a number of ions have been utilized as dopants, including rare earth metals, [8] transition metals [9] and alkaline earth metals [10]. However, unified theory can still be a rather difficult issue, because the property is delicately subject to both strain effect and doping effect. Therefore, systematic study focused on one nanostructure and one doping element is desired. La, Ca singly doped BFO nanofibres have been synthesized previously and studied detailedly [7,11]. They did show enhanced behaviors in magnetic and photocatalytic aspects, however none of these individual dopants was able to modulate the properties ideally and arbitrarily. Given this fact, co-doping has been proposed as an option. Some recent progress in nanofibre preparation [12] has already demonstrated the significance of co-doping and it is hence in urgent need of extensive studies.

In this work, we fixed Mn doping content to 0.05 and varied Ca concentration, in the hope of obtaining one-dimensional BFO nanofibres equipped with more excellent capacity and exploring the interaction between dopants in different doping sites.

2. Experimental

Ca Mn co-doped BFO (Ba_xBi_{1-x}Fe_{0.95}Mn_{0.05}O₃) ultrafine fibres with four Ca doping contents (x = 0, x = 0.05, x = 0.10, x = 0.15) were synthesized through a sol-gel based electrospinning method. Precursor solution was prepared with bismuth nitrate (Bi(NO₃)₃·5H₂O) (5 mol% excess to compensate for Bi loss during the heat treatment in air), iron nitrate (Fe(NO₃)₃·9H₂O), and calcium nitrate (Ca(NO₃)₂·4H₂O) and 50 wt.% manganous nitrate solution (Mn(NO₃)₂). Mixed together with the complexant, citric acid (C₆H₈O₇) in the solvent N, N-Dimethylformamide (DMF, C₃H₇NO), the homogeneous solution was placed in the shade for 24 h aging. Afterwards, polyvinylpyrrolidone (PVP, M = 1,300,000) was added to the mixture solution, which was then continuously stirred till PVP completely dissolved. Subsequently electrospinning process was initiated by loading the ropy precursor solution into a syringe with its stainless-steel needle uploaded with high voltage (13 kV). The rotating cylinder collector 10 cm away was grounded, and a static electric field of

*Corresponding author.

1.3 kV/cm intensity was thus built across. The thick hybrid was squeezed out, drawn into ultrafine nanofibre and started vibrating after going straight a little while, due to the extremely high tension, which prolonged spun duration and assured DMF volatilized thoroughly. The non-volatile, mainly the complex compound, remained on PVP fibres which later weaved on an aluminium foil. These as-spun fibres went through a heating process of 90 min presintering at 420°C, and 3 h calcination at 580°C.

X-ray diffraction (short for XRD) (Rigaku D/max 2500) with Cu K_{α} (0.15418 nm) was utilized to analyze the phase structure. Magnetic behaviors were observed in physical property measurement system (PPMS-9T). Field emission scan electron microscope (FESEM) (JSM-7001F) was employed in the microstructure measurement, and atom arrangement was approached with high resolution transmission electron microscope (HRTEM) (JOEL-2011). Ultraviolet-visible (UV-Vis) curves were tested in Hitachi U3310 spectrophotometer, while photocatalytic performance was carried out under self-made reaction and test system. The degradation of CR was determined by the intensity of the absorption peak of CR (495 nm) relative to its initial value (C/C_0).

3. Result and Discussion

Results of phase structure analysis are shown in **Figure 1**. Some typical peaks for nonstoichiometric phases can be detected, which are possibly from $\text{Bi}_{3.43}\text{Fe}_{0.57}\text{O}_6$ and $\text{Bi}_{25}\text{FeO}_{40}$. Apart from these impurity peaks, all the other could be ascribed to the main phase, BiFeO_3 , JCPDS Card No.86 - 1518. High crystallinity could be proved by the sharp peak shape, and mergers of the doublet peaks, for instance, (104) and (110), (006) and (202), (116) and (122), (214) and (300), indicate a structural transition of space group and symmetry can be obtained by Ca doping, while Mn doping might introduce more impurities, similar phenomenon has been reported previously [13]. As

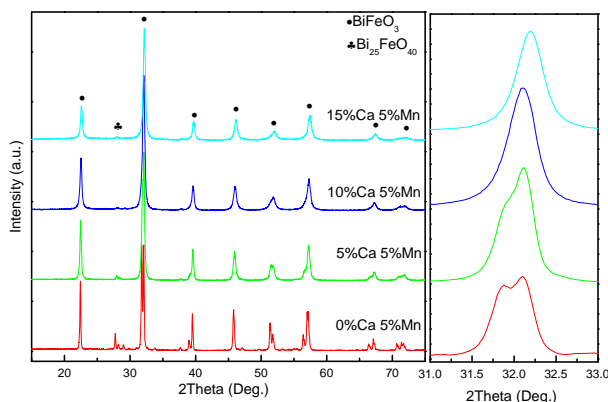


Figure 1. XRD patterns for pristine and doped BFO nanofibres. And slow scan spectra near 32°.

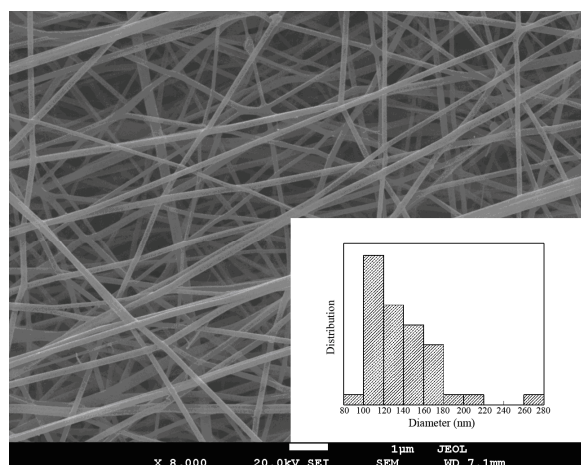
Ca content grows, the peaks shifts to higher angle, indicating the shrinkage of the crystal lattice.

Morphology and microstructure of these nanofibres were observed and the results are shown in **Figure 2**. As spun samples have an average diameter of 140 nm and they are smooth in shape, owing to the polymer nature of carrier PVP. However, after sintering process, the average diameter shrank to below 120 nm and the morphology turned to be coarse. From the HRTEM image, we can find that sunken area might be the grain boundary zone and the adjacent grains stagger quite slightly in crystal orientation probably because of the one-dimensional restraint condition. In the surface area, looser atom arrangement and different lattice plane can be observed, compared with the inside bulk zone.

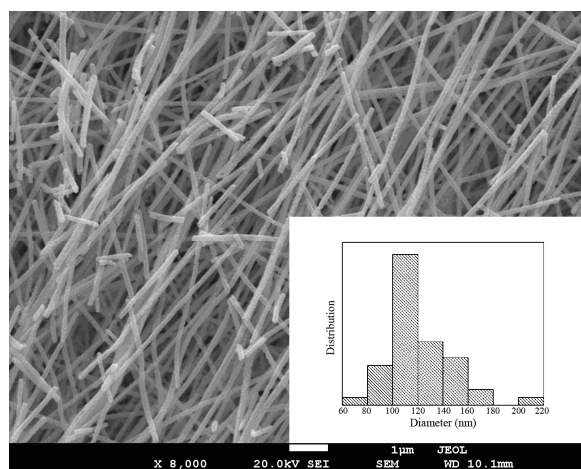
Mn co-doping might endowed these nanofibres enormous impact on the thermal property and structure. In fact, our previous study [11] showed that an annealing temperature of 660°C or a little lower was ideal for singly doped BFO nanofibres. In this co-doping case, we had to reduce the sintering temperature to 580°C to keep the nanofibre shapes unbroken, though Mn concentration was as little as 5%.

Magnetic properties of the as-prepared nanofibres are graphed in **Figure 3**. When Mn is the only dopant, we can see that the fibres show good magnetism with high saturation magnetization, evident remnant magnetization and coercive force. However, when Ca was doped into the fibres, situation changed with a dramatic drop of both saturation magnetization and coercive force. This downgrading trend stops and turns upwards later with incremental Ca content, and when Ca content reaches 10%, saturation magnetization has exceeded that of 5% Mn doped sample. We consider the magnetism of 5% Mn doped fibres to be originated from the magnetic moment of Mn itself, the charge compensation effect and the incident impurity phases. Nevertheless, the pop-in of the Ca might have indirectly conflicted with Mn somehow, for instance, pinned the Mn valence state. Later on, when Ca becomes majority, its impact on Fe becomes dominating. At this moment, the moment of Mn can help strengthen the magnetization instead, together with the Fe valence state variation and $\text{Fe}^{2+}\text{-O-Fe}^{3+}$ super exchange [12,14-16] caused by Ca doping. Our previous work has shown saturation magnetization is positively correlated with the Ca content, [11] while combining with this work, we can infer that Mn should have dual effects, one will be restrained by Ca doping, that is perhaps charge effect, and the other, which is likely to be residual moment, will cooperate with Ca on property improvement.

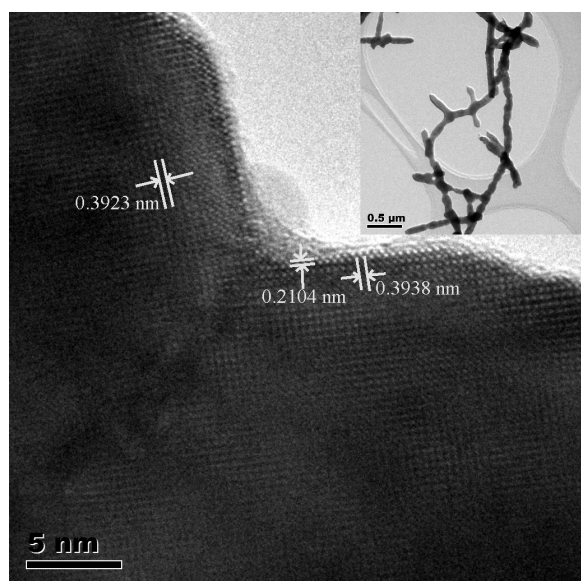
Owing to the superior specific surface area, the catalytic activity is rather worthy to look forward to. Degradation experiment of Congo red has demonstrated the same trend with magnetism variation. As seen from the



(a)

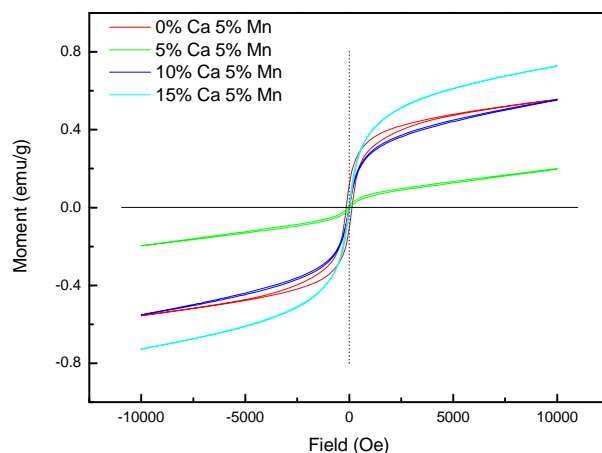


(b)

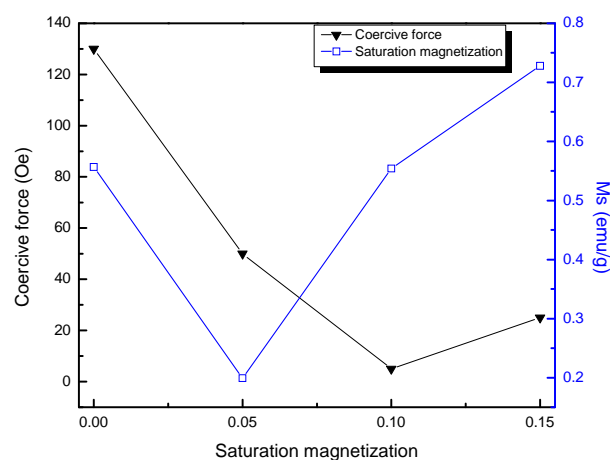


(c)

Figure 2. Morphology and microstructure of BFO nanofibers. SEM image of (a) as spun and (b) sintered sample, and its (c) HRTEM image.



(a)



(b)

Figure 3. (a) M-H curves and (b) magnetic properties in a magnetic field with maximum of 10 k Oe at 300 K (room temperature).

Figure 4, though all samples show good photocatalytic efficiency as a result of considerably large specific surface area and high visible light response, there exists a minimum for photodecomposition. This minimum, arising when the doping concentration is equal, might similarly suggest the mutual weakening effect between Ca and Mn. When Ca doping content is more than 5%, photocatalytic degradation shows positive correlation to doping proportion. And with the co-existence of a small amount of Mn, photocatalytic activity is raised markedly and higher than Ca singly doping. This excellent performance could be explained by increment of free carrier and decreased electron-hole recombination rate, while the excessive activity on the Mn singly doping condition might be attributed to impurity phases and structural influence offered by Mn. In addition, when Mn was brought in the lattice, the bandgap further narrowed down and these nanofibers showed a bit of semi-conductivity, which was consistent with the color change from previous Mn-free samples. We thus assumed that the

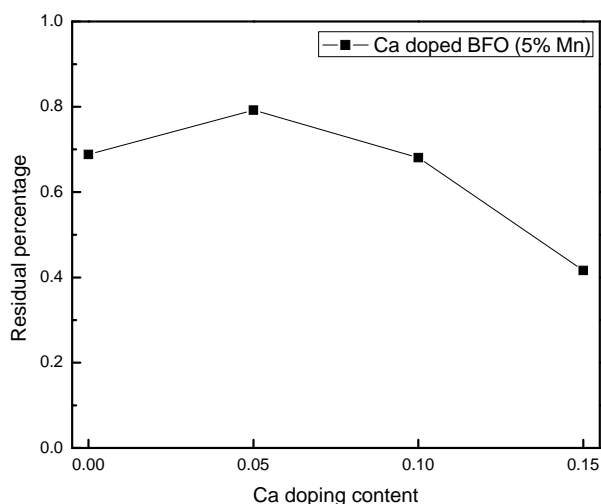


Figure 4. Congo red degradation after 2 h visible light irradiation.

Ca Mn co-doping might bring many states into BFO and therefore had immense impact on the catalytic behavior.

4. Conclusion

In conclusion, the influence of Ca Mn co-doping on phase structure, magnetic and photocatalytic properties of BFO nanofibres was systematically investigated. Mn doping has triggered some impurity which can later be suppressed by Ca doping, and in this process, a space group transition can be observed. Magnetic and photocatalytic measurement suggested a dual role of Mn, and by this co-doping method, the performances can be enhanced and modulated.

5. Acknowledgements

This work was supported by the Ministry of Science and Technology of China through a 973-Project under Grant No. 2009CB623303, NSF of China (51272121 and 5102 5205).

REFERENCES

- [1] G. A. Smolenskii and I. Chupis, "Ferroelectromagnets," *Soviet Physics Uspekhi*, Vol. 25, No. 7, 1982, pp. 475-493. [doi:10.1070/PU1982v025n07ABEH004570](https://doi.org/10.1070/PU1982v025n07ABEH004570)
- [2] T. Choi, S. Lee, Y. J. Choi, V. Kiryukhin and S. W. Cheong, "Switchable Ferroelectric Diode and Photovoltaic Effect in BiFeO₃," *Science*, Vol. 324, No. 5923, 2009, pp. 63-66. [doi:10.1126/science.1168636](https://doi.org/10.1126/science.1168636)
- [3] J. Wang, J. B. Neaton, H. Zheng, V. Nagarajan, S. B. Ogale, B. Liu, D. Viehland, V. Vaithyanathan, D. G. Schlom, U. V. Waghmare, N. A. Spaldin, K. M. Rabe, M. Wuttig and R. Ramesh, "Epitaxial BiFeO₃ Multiferroic Thin Film Heterostructures," *Science*, Vol. 299, No. 5613, 2003, pp. 1719-1722. [doi:10.1126/science.1080615](https://doi.org/10.1126/science.1080615)
- [4] F. Gao, X. Y. Chen, K. B. Yin, S. Dong, Z. F. Ren, F. Yuan, T. Yu, Z. G. Zou, J. M. Liu and Adv. Mater, "Visible-Light Photocatalytic Properties of Weak Magnetic BiFeO₃ Nanoparticles," Vol. 19, No. 19, 2007, pp. 2889-2892. [doi:10.1002/adma.200602377](https://doi.org/10.1002/adma.200602377)
- [5] S. Li, Y. H. Lin, B. P. Zhang, Y. Wang and C. W. Nan, "Controlled Fabrication of BiFeO₃ Uniform Microcrystals and Their Magnetic and Photocatalytic Behaviors," *The Journal of Physical Chemistry C*, Vol. 114, No. 7, 2010, pp. 2903-2908. [doi:10.1021/jp910401u](https://doi.org/10.1021/jp910401u)
- [6] X. Xu, Y. H. Lin, P. Li, L. Shu and C. W. Nan, "Synthesis and Photocatalytic Behaviors of High Surface Area BiFeO₃ Thin Films," *Journal of the American Ceramic Society*, Vol. 94, No. 8, 2011, pp. 2296-2299. [doi:10.1111/j.1551-2916.2011.04653.x](https://doi.org/10.1111/j.1551-2916.2011.04653.x)
- [7] Z. A. Zhang, H. Y. Liu, Y. H. Lin, Y. Wei, C. W. Nan and X. L. Deng, "Influence of La Doping on Magnetic and Optical Properties of Bismuth Ferrite Nanofibers," *Journal of Nanomaterials*, Vol. 2012, No. 238605, 2012, pp. 1-5. [doi:10.1155/2012/238605](https://doi.org/10.1155/2012/238605)
- [8] J. Liu, L. Fang, F. Zheng, S. Ju and M. Shen, "Enhancement of magnetization in Eu doped BiFeO₃ nanoparticles," *Applied Physics Letters*, Vol. 95, No. 2, 2009, pp. 022511-022513. [doi:10.1063/1.3183580](https://doi.org/10.1063/1.3183580)
- [9] P. Kharel, S. Talebi, B. Ramachandran, A. Dixit, V. M. Naik, M. B. Sahana, C. Sudakar, R. Naik, M. S. R. Rao and G. Lawes, "Structural, Magnetic, and Electrical Studies on Polycrystalline Transition-Metal-Doped BiFeO₃ Thin Films," *Journal of Physics: Condensed Matter*, Vol. 21, No. 3, 2009, pp. 036001-036006. [doi:10.1088/0953-8984/21/3/036001](https://doi.org/10.1088/0953-8984/21/3/036001)
- [10] B. Bhushan, A. Basumallick, S. K. Bandopadhyay, N. Y. Vasanthacharya and D. Das, "Effect of Alkaline Earth Metal Doping on Thermal, Optical, Magnetic and Dielectric Properties of BiFeO₃ Nanoparticles," *Journal of Physics D: Applied Physics*, Vol. 42, No. 6, 2009, pp. 065004-065011. [doi:10.1088/0022-3727/42/6/065004](https://doi.org/10.1088/0022-3727/42/6/065004)
- [11] Y. N. Feng, H. C. Wang, Y. D. Luo, Y. Shen and Y. H. Lin, "Ferromagnetic and Photocatalytic Behaviors Observed in Ca-Doped BiFeO₃ Nanofibres," *Journal of Applied Physics*, Vol. 113, No. 14, 2013, pp. 146101-146103. [doi:10.1063/1.4801796](https://doi.org/10.1063/1.4801796)
- [12] B. Li, C. Wang, W. Liu, M. Ye and N. Wang, "Multiferroic Properties of La and Mn Co-Doped BiFeO₃ Nanofibers by Sol-Gel and Electrospinning Technique," *Materials Letters*, Vol. 90, 2013, pp. 45-48. [doi:10.1016/j.matlet.2012.09.012](https://doi.org/10.1016/j.matlet.2012.09.012)
- [13] H. C. Wang, Y. H. Lin, Y. N. Feng and Y. Shen, "Photocatalytic Behaviors Observed in Ba and Mn Doped BiFeO₃ Nanofibers," *Journal of Electroceramics*, 2013, pp. 1-4. [doi:10.1007/s10832-013-9818-8](https://doi.org/10.1007/s10832-013-9818-8)
- [14] J. Wei and D. Xue, "Effect of Non-Magnetic Doping on Leakage and Magnetic Properties of BiFeO₃ Thin Films," *Applied Surface Science*, Vol. 258, No. 4, 2011, pp. 1373-1376. [doi:10.1016/j.apsusc.2011.09.066](https://doi.org/10.1016/j.apsusc.2011.09.066)
- [15] F. P. Gheorghiu, A. Ianculescu, P. Postolache, N. Lupu, M. Dobromir, D. Luca and L. Mitoseriu, "Preparation and Properties of (1 - x)BiFeO₃ - xBaTiO₃ Multiferroic Ceramics," *Journal of Alloys and Compounds*, Vol. 506, No. 2, 2010, pp. 862-867. [doi:10.1016/j.jallcom.2010.07.098](https://doi.org/10.1016/j.jallcom.2010.07.098)

- [16] Y. Wang and C. W. Nan, "Enhanced Ferroelectricity in Ti-Doped Multiferroic BiFeO₃ Thin Films," *Applied Physics Letters*, Vol. 89, No. 5, 2006, pp. 052903-052905. [doi:10.1063/1.2222242](https://doi.org/10.1063/1.2222242)